ACS OMEGA

Article

Cite This: ACS Omega 2020, 5, 995−1002

Cancer Cell Membrane-Decorated Zeolitic-Imidazolate Frameworks Codelivering Cisplatin and Oleanolic Acid Induce Apoptosis and Reversed Multidrug Resistance on Bladder Carcinoma Cells

Dong Chen,[†] Longbo Cai,[†] Yihong Guo,[†] Junyi Chen,[†] Qiangli Gao,[‡] Junxian Yang,[‡] and Yongfa Li*[,‡]

[†]Department of Urology, 2nd Affiliated Hospital of Fujian Medical University, Quanzhou City 362000, Fujian Province, China

[‡]Department of Urology, The Affiliated Puren Hospital of Wuhan University of Science and Technology, No. 1 Benxi Street, the Fourth Jianshe Road, Qingshan District, Wuhan 430080, China

ABSTRACT: Combination therapy is emerging as a preferable approach in cancer therapy with minimized side effects and elevated performance. Nevertheless, the poor targeting and drug loading of currently available drug delivery systems (DDSs) are the main difficulties to realize preferable combination therapy of cancer. As a result, a cancer cell membrane-decorated zeolitic-imidazolate framework hybrid nanoparticle (HP) was successfully constructed in our study to codeliver cisplatin (DDP) and oleanolic acid (OLA). Our results showed positive results of the platform (HP/DDP/OLA) for the treatment of bladder cancer (SW780). In detail, HP/DDP/OLA could enhance apoptosis while reverse multidrug resistance in SW780 cells than free drugs alone or monodelivery systems, which might be a suitable DDS for codelivery of different drugs with great promise.

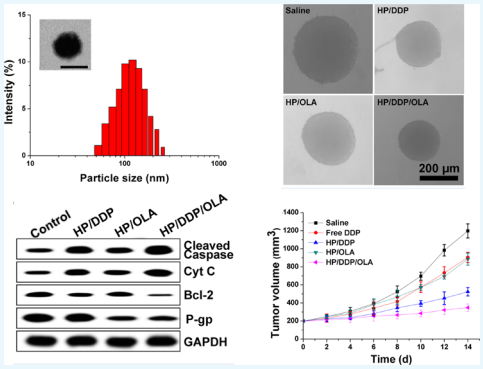

1. INTRODUCTION

At present, cancer chemotherapy is still the most widely adopted approach for cancer therapy.[1−3] However, because of the developed multidrug resistance (MDR) in various types of cancer, the administration of a single drug molecule usually fails to effectively control the progress of cancers.[4,5] Hence, the combined administration of different types of drugs gradually emerged to be an alternative for better performance in cancer therapy.[6,7] Previous studies have demonstrated that combination therapy could greatly enhance the cytotoxicity while reducing the dosage, which significantly reduces the unwanted side effects of anticancer drugs. The basic principle for combination therapy is to codeliver at least two drugs targeting different pathways, which ensure the high cytotoxicity to cancer cells.[8,9] However, the combination therapy greatly relies on the assistance of drug delivery systems (DDSs) to precisely control the dosage, proportion, and even the sequence of loaded cargos. Considering that most of the currently adopted DDSs are not able to satisfy the first two basic requirements, the introduction of a well-designed DDS is the prerequisite for effective combination therapy.[2]

Over the past decades, the development of a novel DDS suitable for cancer therapy is the research hotspot of pharmaceutical science. Various DDSs based on different materials have been developed to test their feasibility in cancer therapy.[10−12] In particular, the outstanding merits of zeolitic-imidazolate framework (ZIF) nanoparticles, including high biocompatibility, low cost, and decent drug loading of different drugs (from hydrophilic to hydrophobic), have made it suitable for the chemotherapy of cancers.[13,14] Apart from the carriers, the tumor-homing capability of the resulted DDS is another important issue that should be taken into consideration because the availability of drugs is largely dependent on the tumor targetability of the DDS.[15] In recent years, cancer cell membrane (CCM) with the combination of shielding and targeting has become the most widely studied material. CCM-modified DDSs were found to smartly home the isogenous cancer cells with high efficiency, while at the same time they can significantly alleviate the liver capture.[16,17]

Cisplatin (DDP) is one of the most commonly adopted drugs for the chemotherapy of various cancers.[18] The mechanism for the DDP-induced anticancer effect is to form DDP−DNA adducts and hinder DNA transfection. However, the drug resistance for DDP has been developed in various types of cancer, as confirmed by many clinical observations. Moreover, the severe side effects of DDP are also another concern, which hampered its performance in many clinical trials. As a result, combination therapy is believed to be an ideal regimen to minimize the MDR of tumor cells and to reduce the DDP-related toxic effects.[19,20]

Oleanolic acid (OLA) is one of the most abundant triterpenoids in plants, which is known for its critical potentials in regulating many pharmacological processes, especially the antitumor activity.[21] It has been demonstrated that the anticancer activity of OLA is realized through the activation of the AMP-activated protein kinase (AMPK) pathway,

Received: July 22, 2019
Accepted: September 11, 2019
Published: January 6, 2020

DOI: 10.1021/acsomega.9b02261
ACS Omega 2020, 5, 995−1002

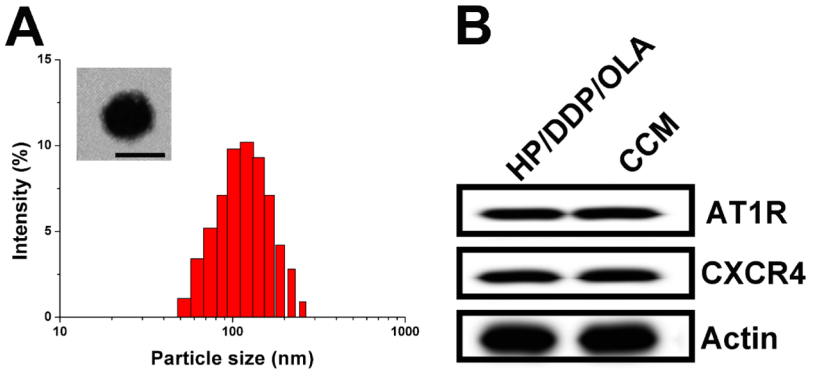

Figure 1. (A) Size distribution of HP/DDP/OLA. The inset shows TEM observation of HP/DDP/OLA. Scale bar: 100 nm. (B) Comparative AT1R and CXCR4 proteins in HP/DDP/OLA and bare CCM.

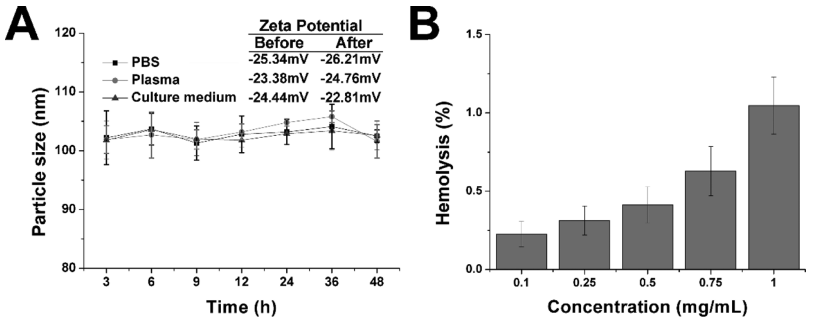

Figure 2. (A) Time-dependent size changes of HP/DDP/OLA in PBS, plasma, and culture medium for 48 h. The inset shows the zeta potential of HP/DDP/OLA before and after incubation in PBS, plasma, and culture medium for 48 h. (B) Concentration-dependent hemolysis of HP/DDP/OLA against 2% RBCs. Data were repeated thrice and expressed as standard deviation.

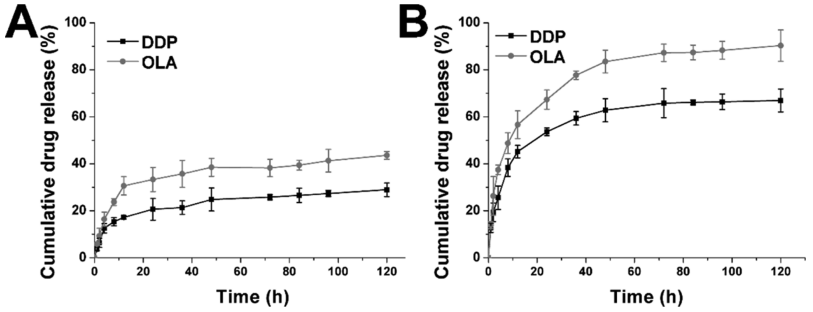

Figure 3. Drug release of DDP and OLA from HP/DDP/OLA at the pH of 7.4 (A) and 5.5 (B). Data were repeated thrice and expressed as standard deviation.

suppression of the P13K-AKT-mTOR-NF-κB pathway, and upregulation of p53 activation and the apoptosis pathway. In recent studies, OLA has been reported to achieve elevated outcome with enhanced apoptosis and reduced side effects when applied with other chemotherapy reagents.[22,23]

Here, in our study, we choose DDP and OLA for combination therapy because of their distinguished mechanisms in cancer therapy. CCM-decorated ZIF as a hybrid nanoparticle (HP) was employed as the delivery vehicle to load both drugs in the same system to finally construct a DDS for the chemotherapy of bladder carcinoma.

2. RESULTS AND DISCUSSION

The preparation of HP/DDP/OLA contained two successive steps. First, the ZIF was prepared using a previous reported coprecipitation method, during which both drugs (DDP and OLA) were loaded into the core of ZIF to obtain a dual-loaded core. The loaded ratio of drugs can be carefully tuned by the charged ratio. Most importantly, the abundant Zn^{2+} on the surface of ZIF can serve as a linker to react with the phosphate groups of our CCM, which resulted in facile anchoring of CCM on the surface of ZIF to offer protection, stabilization, and targeting for the DDS. As shown in Figure 1A, the size distribution of HP/DDP/OLA was uniformly distributed at around 100 nm with a small polydispersion index of 0.086. The transmission electron microscopy (TEM) image given in the inset also confirmed this conclusion. In addition, the western blot analysis of CCM and HP/DDP/OLA revealed similar protein components, with comparable AT1R and CXCR4 detected, which provided decisive evidence to prove that CCM was successfully anchored to the corona of HP/DDP/OLA (Figure 1B).

Afterward, the stability of HP/DDP/OLA was studied to reveal the suitability to serve as a DDS. As shown in Figure 2A,

DOI: 10.1021/acsomega.9b02261
ACS Omega 2020, 5, 995−1002

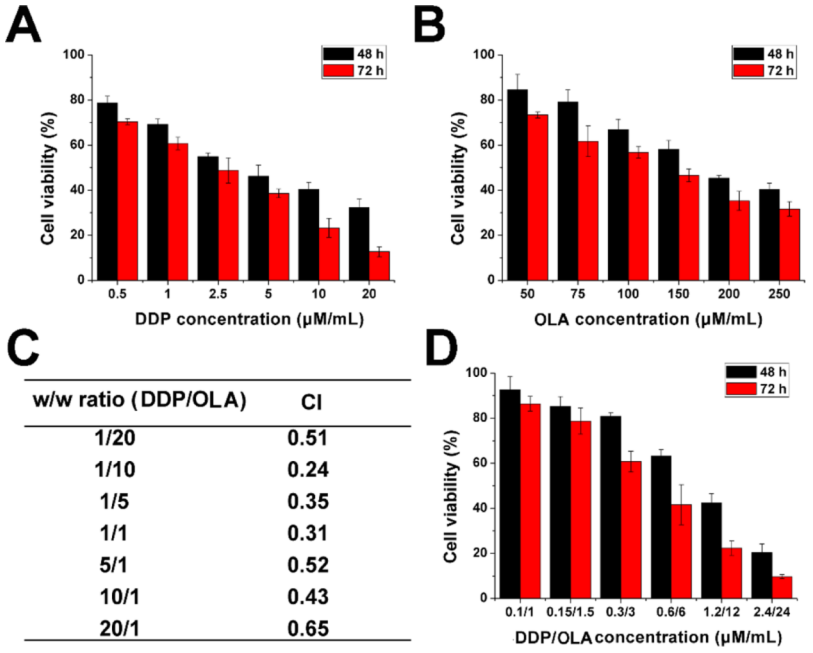

w/w ratio (DDP/OLA)	CI
1/20	0.51
1/10	0.24
1/5	0.35
1/1	0.31
5/1	0.52
10/1	0.43
20/1	0.65

Figure 4. Cell viability revealed by the MTT assay after SW780 cells treated with HP/DDP or HP/OLA at different DDP (A) or OLA (B) concentrations for 48 and 72 h. (C) CI of HP/DDP/OLA-treated SW780 cells for 72 h at different DDP/OLA ratios (w/w). (D) In vitro anticancer effect of HP/DDP/OLA (DDP/OLA = 10, w/w) at different drug concentrations. Data were repeated thrice and expressed as standard deviation.

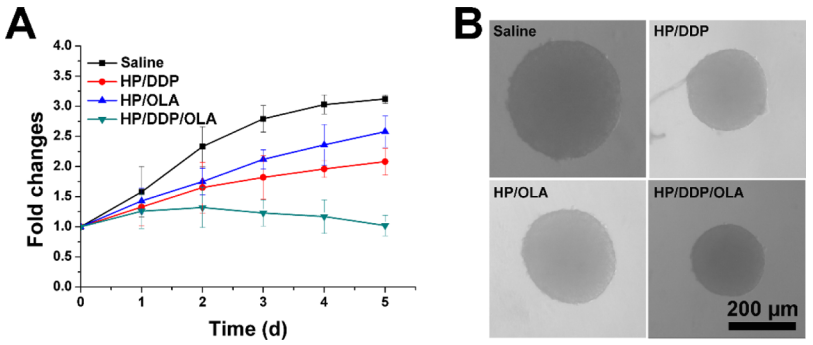

Figure 5. Volume variations (A) and optical images (B) of MCTS treated with different formulations. Data were repeated thrice and expressed as standard deviation. Scale bar: 200 μm.

although being incubated in three different solutions, the changes of particle size in HP/DDP/OLA were not significant. Moreover, the zeta potential measurement in all three media also revealed insignificant changes before and after incubation. The results indicated the preferable stability of HP/DDP/OLA under physiological conditions, which satisfied the primary requirement to serve as a DDS. Moreover, the hemolysis as another parameter for biocompatibility was also investigated to reveal the safety of HP/DDP/OLA. As shown in Figure 2B, the HP/DDP/OLA showed a concentration-dependent hemolysis on red blood cells (RBCs). However, it was noted that at the highest concentration of 1 mg/mL, the hemolysis of HP/DDP/OLA was lower than 1%, which was much below the warning level of 5%. On the other hand, it was reported that nanoparticles administered intravenously will be dramatically diluted by the circulating blood, which was several orders of magnitude lower than the tested ones. As a result, it was concluded from the results that HP/DDP/OLA was highly biocompatible to be a DDS.[24]

The drug release profile of HP/DDP/OLA under physiological and pathological environments was studied. As shown in Figure 3A,B, under physiological conditions (pH 7.4), both DDP and OLA were released slowly from the DDS, with 33.2.6% of OLA and 25.4% of DDP being released at 120 h post incubation. In contrast, in the pathological environment, the drug release was significantly elevated, which was 90.8 and 69.6% for OLA and DDP, respectively. The significantly increased drug release might be due to the pH-responsive decomposition nature of ZIF, which was beneficial for effective cancer therapy because most of the tumor tissues were well recognized to be more acidic than normal environments.

Next, the in vitro anticancer benefit of HP/DDP/OLA was studied using the methyl thiazolyl tetrazolium (MTT) assay. As shown in Figure 4A,B, the mono delivery system showed certain benefits on SW780 cells as supported by the concentration-dependent decrease of cell viability. The calculated IC50 values for DDP alone were 4.21 μM (48 h) and 2.38 μM (72 h), respectively. The IC50 values for OLA were calculated to be 183 μM (48 h) and 142 μM (72 h),

DOI: 10.1021/acsomega.9b02261
ACS Omega 2020, 5, 995−1002

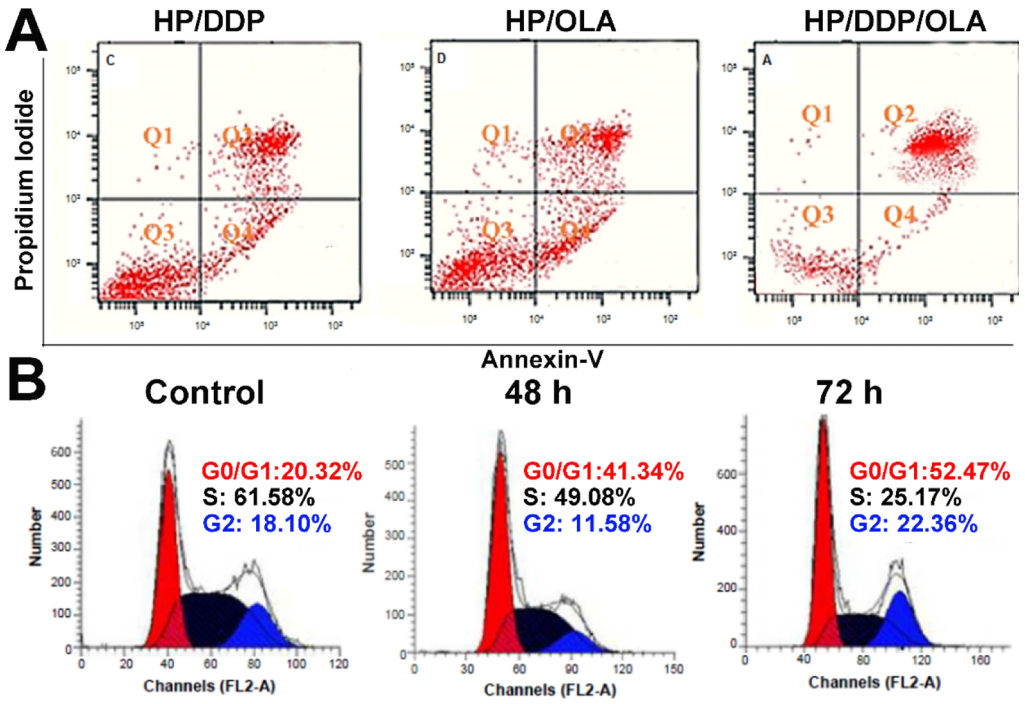

Figure 6. (A) Apoptosis of SW780 cells treated with different formulations at the drug concentration of 0.89/8.9 μM for 72 h. (B) Cell cycle variations of SW780 cells treated with HP/DDP/OLA for different time intervals. Data were repeated thrice and expressed as standard deviation.

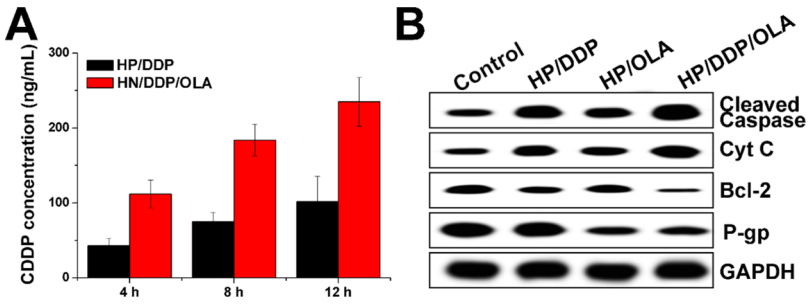

Figure 7. (A) Intracellular drug concentration of SW780 cells treated with different formulations for different time intervals. Data were repeated thrice and expressed as standard deviation. (B) Western blot assay of protein variations after SW780 cells were treated with different formulations for 72 h. Data were repeated thrice and expressed as standard deviation.

respectively. In order to find the optimal ratio for the combination therapy, the relation between drug ratios (DDP/OLA, w/w) and combination index (CI) was summarized. As demonstrated in Figure 4C, it was concluded that at the w/w ratio of 10, the CI was the lowest, which indicated that the combination effect of the drugs was optimal. As a result, the following MTT assay was tested using this ratio unless otherwise stated. The MTT assay at this ratio was further tested under the optimal drug ratio. As illustrated in Figure 4D, compared to free DDP or OLA, the combination of DDP and OLA can greatly reduce the dosage when achieving the same cytotoxicity. The IC50 was achieved at the dosage of 1.58/15.8 μM for 48 h and 0.82/8.2 μM for 72 h. From the results of the above experiments, it was clearly demonstrated that the combination of DDP and OLA was able to greatly increase the anticancer benefit at a low dosage.

In order to further confirm this conclusion, the MCTS model was further employed to test the anticancer effect of different formulations. As shown in Figure 5A, mono delivery systems only demonstrated moderate benefits in cancer therapy, while the codelivery of both drugs was demonstrated to greatly evaluate the performance, which finally resulted in reverse in MS volume as compared to other groups. The pictures captured at the end of the assay in Figure 5B also reached similar conclusions.

Next, with the aim to test the mechanisms responsible for the elevated anticancer benefit, the apoptosis in different formulations was investigated. As demonstrated in Figure 6A, at 72 h post incubation under the same drug concentration (0.82/8.2 μM), the HP/DDP group showed 43.6% of apoptosis, whereas HP/OLA showed only 31.4% of apoptosis. In contrast, the apoptosis in the HP/DDP/OLA group was significantly elevated to 72.3% under the same condition. The investigation of changes in cell cycles also revealed interesting results. As displayed in Figure 6B, the combination therapy of HP/DDP/OLA revealed that the synergetic effects of both drugs were able to increase the arrest in the G0/G1 phase and reduce the percentage of the S phase. More importantly, the effect was positively related to the incubation time. It was widely recognized that the S phase indicated the division of cells, the arrest in the G0/G1 phase and reduction in the S

DOI: 10.1021/acsomega.9b02261
ACS Omega 2020, 5, 995−1002

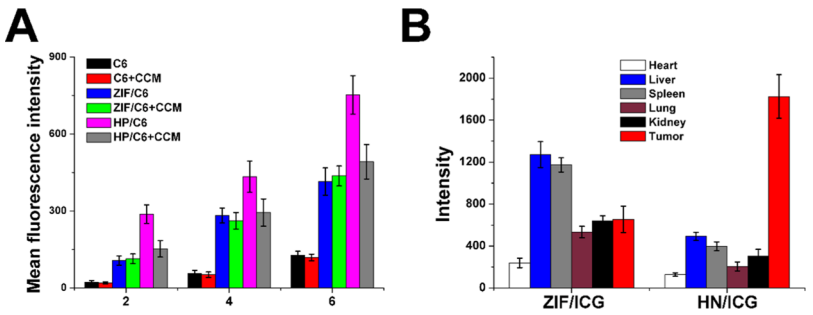

Figure 8. In vitro (A) and in vivo (B) targeting assays of HP/DDP/OLA. Data were repeated thrice and expressed as standard deviation.

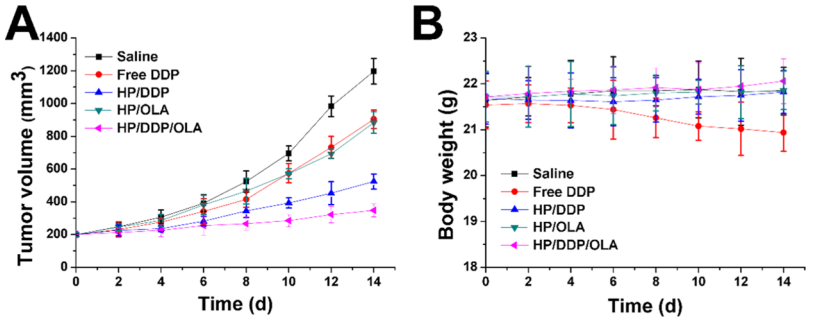

Figure 9. Tumor volume (A) and body weight (B) variations of SW780 tumor-bearing mice treated with different formulations. Data were expressed as standard deviation.

phase, both indicating the impaired proliferation of cancer cells, which was beneficial in cancer therapy.

Moreover, the reverse of MDR in SW780 cells was further explored by investigating the intracellular time-dependent drug accumulation of DDP. As shown in Figure 7A, compared with the mono delivery system, the codelivery of DDP and OLA resulted in enhanced drug accumulation in cells, which was positively related to the incubation time. As a result, it was suggested that the integration of OLA into the DDS could significantly reverse the MDR in SW780 cells, which was beneficial for the accumulation of DDP in cells for better performance. Afterward, the variations of cellular protein levels were detected using western blot to illuminate the reasons responsible for the reverse of MDR. As shown in Figure 7B, it was interesting to note that the mono delivery of DDP was able to trigger P-gp overexpression in SW780 cells, which was in line with the previous report that chemotherapy was responsible for the acquired MDR in cancer cell lines. Most importantly, the treatment of OLA-containing formulations significantly reduced the expression of P-gp proteins in SW780 cells as compared to the that of the OLA-deficient group, which were comparable in downregulating the P-gp levels. Therefore, it was inferred that OLA could effectively reverse the MDR induced by DDP through the downregulation of P-gp expression.[25,26]

Next, the in vitro and in vivo targeting of HP was studied. The time-dependent and competitive cellular uptake was first adopted to study the in vitro targeting of HP. C6 was integrated into the DDS to be an indicator to reveal the uptake profile of different nanoparticles. As demonstrated in Figure 8A, it was clearly observed that the intracellular uptake of all formulations was positively related to the incubation time, which suggested that extended incubation resulted in higher accumulation of nanoparticles within cells. However, free C6 showed relatively slow accumulation in cells, which indicated that free drugs with the hydrophobic nature could be hardly uptaken by the cells. Most importantly, the cells treated with nanoparticles showed elevated C6 signal in cells, which was consistent with previous reports that nanoparticles could facilitate the internalization of drugs into cells.[27,28] Moreover, it was noted that the fluorescence intensity of the HP-treated group was 1.83-fold higher than that of the ZIF-treated group after incubation for 6 h, which suggested the possibility of preferable uptake of HP in SW780 cells. In order to verify this suggestion, the comparative experiment was conducted using free CCM as the competitor. After exposure to excess of CCM for 2 h, the intracellular C6 signals in different groups were recorded and compared. As expected, the intracellular uptake of HP suffered serious decline in SW780 cells after CCM pretreatment, while insignificant changes were shown in ZIF-treated SW780 cells. These phenomena strongly suggested that the surface-anchored CCM was involved in the variations of cellular uptake between different formulations, which suggested that CCM modification might be able to guide the DDS to homologous cells with the same membrane components.[29]

Surface decoration of CCM was shown to promote the accumulation of DDS in SW780 cells. Whether this effect could be realized in living lives was also investigated to show the potential of HP for in vivo application. As shown in Figure 8B, ZIF and HP were labeled with ICG and then injected intravenously to the SW780 xenografted mice. At 24 h post nanoparticle administration, the mice were sacrificed to harvest the organs and tumor to determine the fluorescence signals using ex vivo imaging. In line with results in Figure 8A, the HP/ICG group showed 2.91-fold of fluorescence signal in tumor compared with that in the ZIF/ICG group, while the intensity in liver was only 23.5% of the ZIF/ICG group. The above observations clearly demonstrated that the tumor-targeting nature of CCM could not only realize enhanced cellular uptake on the cellular level but also was capable of

DOI: 10.1021/acsomega.9b02261
ACS Omega 2020, 5, 995−1002

guiding the HP to accumulate in the in vivo tumor tissue with reduced capture by the liver.[30,31]

Eventually, the in vivo antitumor efficacy of the DDS was assessed using the SW780 xenografted model. The changes in tumor growth and body weight were recorded twice a day before drug administration in detail. As shown in Figure 9A, in line with the MTT assay, the anticancer performance of different formulations followed the order of HP/DDP/OLA > HP/DDP > HP/OLA ≈ free DDP. From these results, we were able to conclude that DDS was capable of effectively delivering the drug for enhanced anticancer outcome because the anticancer effect of HP/DDP was much better than that of free DDP. Most importantly, the in vivo experiments further confirmed that the combination therapy of DDP was much more superior to the mono therapy. In addition, the variations of body weight in Figure 9B also gave some interesting information. First of all, it was realized that free DDP without the aid of DDS was not suitable for cancer therapy because it caused severe loss of body weight during the test, which suggested that the side effect of DDP significantly impaired the health of the subjects.[32] In contrast, with the help of DDS, HP/DDP showed almost no adverse effects on the subjects, which was comparable to that of HP/DDP/OLA. In all, it was suggested that HP/DDP/OLA was a highly biocompatible DDS with significantly elevated anticancer benefits than mono delivery systems.[33,34]

3. CONCLUSIONS

In our study, we have fabricated a multifunctional DDS capable of delivering DDP and OLA in the same platform for synergetic chemotherapy of bladder carcinoma (HP/DDP/OLA). The results revealed that HP/DDP/OLA was a stable DDS with high biocompatibility. Moreover, HP/DDP/OLA showed pH responsiveness with preferable tumor targeting. Most importantly, the in vitro and in vivo anticancer benefits of HP/DDP/OLA were both greatly elevated as compared to mono delivery systems, which could reverse the MDR and increase the apoptosis and cell arrest of treated cancer cells.

4. EXPERIMENTAL SECTION OR COMPUTATIONAL METHODS

4.1. Materials, Cells, and Animal Model. All chemical reagents were of analytical pure grade and from Sigma-Aldrich (St. Louis, MO, USA). The SW780 and NIH3T3 cells were cultured in Dulbecco's modified Eagle's medium supplied with 10% fetal bovine serum. The multicellular tumor spheroid (MCTS) model was established using the previous protocol. In brief, equal number of SW780 and NIT3T3 cells was mixed and seeded on 96-well plates (Corning, USA), which were then allowed to grow into MCTS.[13] Male BALB/c nude mice were subjected to tumor implantation according to the previous report. SW780 was collected and dispersed in phosphate-buffered saline (PBS) to reach an intensity of 2×10^7 cells/mL and injected to the flank of mice (100 μL) to allow tumor formation.[35]

4.2. Preparation of DDS. $Zn(NO_3)_2{\cdot}6H_2O$, DDP, and OLA were dissolved 10 mL of ethanol at room temperature under gentle stirring to obtain a clear solution. Afterward, the methanol solution of 2-methylimidazole was quickly charged into the ethanol solution of the mixture with vigorous stirring for 30 s. Afterward, the mixture was allowed to stand at room temperature for 30 min to remove the large aggregates. The supernatant was then centrifuged (3000 rpm, 10 min) to obtain the homogeneous nanoparticles loaded with both drugs (ZIF/DDP/OLA). Nanoparticles loaded with a single drug were also prepared using the similar protocol.[36]

The CCM was isolated from SW780 cells using previously reported procedures. Briefly, cells were subjected to repeated freezing and thawing 6 times. Afterward, the mixture was centrifuged (3000 rpm, 10 min) to obtain the supernatant (4 °C). Finally, the supernatant was processed by an extruder equipped with a 0.22 μm membrane several times to obtain the CCM (4 °C). The protein in CCM was quantified by the BCA kit (Beyotime, China).[37]

For the coating of CCM to ZIF to construct HP/DDP/OLA, the aqueous solution of ZIF (1 mg/mL) was mixed with different ratios of CCM by vortexing. After being sonicated for half an hour (100 W), HP HP/DDP/OLA was obtained by centrifuging the mixture at 10 000g for 10 min.

4.3. Characterization. The particle size distribution and zeta potential of nanoparticles were assessed by the particle/zeta measuring system (Zetasizer Nano ZS, Malvern, UK). The morphology was observed by TEM (Hitachi HF5000, Hitachi, Japan).

4.4. Stability and Hemolysis. The stability of HP/DDP/OLA was evaluated by measuring the size changes of nanoparticles in PBS and plasma for 48 h. The hemolysis of HP/DDP/OLA was evaluated by determining the UV absorbance (545 nm) of the supernatant (2% RBCs of mouse blood) after treated with different concentrations of HP/DDP/OLA.

4.5. Drug Loading and Drug Release. The platinum content in DDS was determined by atomic absorption spectroscopy (iCE 3500, Thermos-Fisher, USA). The content of OLA was measured by high-performance liquid chromatography (LC-2030, Shimadzu, Japan) with the following conditions: Agilent SB-C18 880975-902 column (4.6 mm, 250 mm, 5 μm); mobile phase was 0.1% trifluoroacetyl aqueous solution: acetonitrile/methanol mixture (17:1) = 1:9. The temperature was 30 °C, the flow rate was 1 mL/min, and the detection wavelength was 210 nm.[38]

4.6. In Vitro Anticancer Assay. Cells were cultured in 96-well plates and treated with different formulations at different drug concentrations for 48 or 72 h. At the predetermined time interval, a standard MTT assay was applied as previously reported. To determine their synergistic effect, the CI was calculated as previously reported.[39]

MCTS was subjected to the treatment of different formulations for 4 days. The changes in MCTS volume were recorded and plotted against time.

4.7. Apoptosis and Cell Cycle. The cells were treated with the apoptosis kit and cell cycle kit (Solabio, China) according to the manufacturer's instructions. Afterward, the cells were subjected to fluorometric analysis using flow cytometry (ACEA NovoCyte, China).

4.8. Intracellular Uptake and Western Blot. Cells were treated with different formulations for different time intervals. At predetermined time intervals, cells were collected and washed, followed by lysis to fully extract the intracellular DDP. Finally, the DDP content was determined as described above.

Cells treated with different formulations for 48 h were collected and lysed by the radioimmunoprecipitation assay buffer. The supernatant was collected and loaded onto the sodium dodecyl sulfate-polyacrylamide gel electrophoresis gel for protein separation. Afterward, the proteins were transferred

DOI: 10.1021/acsomega.9b02261
ACS Omega 2020, 5, 995−1002

to another poly(vinylidene difluoride) membrane to allow the label of corresponding antibodies. The proteins were revealed by a chemiluminescence imager (Invitrogen iBright, ThermoFisher, USA).

4.9. Tumor-Targeting Assay. Coumarin-6 was encapsulated into CCM and then employed to construct the DDS. The C6-labeled DDS was then used to study the in vitro cellular uptake of DDS. In brief, cells were pretreated with CCM or PBS for 2 h, followed by incubation with different formulations for different time intervals. At each interval, cells were collected and subjected to flow cytometry analysis of intracellular fluorescence intensity.

To study the in vivo tumor targeting of DDS, DiR was loaded instead of C6 and the DiR-labeled DDS was injected into the SW780 tumor-bearing mice through the tail vein. At 24 h post administration, the mice were executed to harvest organs and tumor tissues and then subjected to fluorometric analysis of intensity by the imaging equipment (Bio-Real, Geneway, Austria).

4.10. In Vivo Anticancer Efficacy. Tumor-bearing mice were selected and randomly grouped into five teams ($n = 6$). The mice were treated with different formulations at the DDP dosage of 7.5 mg/kg and OLA dosage of 20 mg/kg via tail vein injection. The measurement of tumor volume and body weight was repeated 7 times before drug administration once every 2 days.

AUTHOR INFORMATION

Corresponding Author

*E-mail: yongfali01@tom.com.

ORCID

Yongfa Li: 0000-0002-7328-0731

Notes

The authors declare no competing financial interest.

ACKNOWLEDGMENTS

We acknowledge the financial support from Youth Research Project, Health and Family Planning Commission, Fujian Province, China, 2015 (grant no. 2015-1-59) and Science and Technology Planning Project, Quanzhou City, 2016 (grant no. 2016Z044).

REFERENCES

(1) Wang, C.; Wang, Z.; Zhao, X.; Yu, F.; Quan, Y.; Cheng, Y.; Yuan, H. DOX Loaded Aggregation-induced Emission Active Polymeric Nanoparticles as a Fluorescence Resonance Energy Transfer Traceable Drug Delivery System for Self-indicating Cancer Therapy. *Acta Biomater.* **2019**, *85*, 218−228.

(2) Meng, Z.; Zhou, X.; Xu, J.; Han, X.; Dong, Z.; Wang, H.; Zhang, Y.; She, J.; Xu, L.; Wang, C.; Liu, Z. Light-Triggered In Situ Gelation to Enable Robust Photodynamic-Immunotherapy by Repeated Stimulations. *Adv. Mater.* **2019**, *31*, 1900927.

(3) Xiong, H.; Ni, J.; Jiang, Z.; Tian, F.; Zhou, J.; Yao, J. Intracellular self-disassemble polysaccharide nanoassembly for multi-factors tumor drug resistance modulation of doxorubicin. *Biomater. Sci.* **2018**, *6*, 2527−2540.

(4) Negi, L. M.; Talegaonkar, S.; Jaggi, M.; Verma, A. K. Hyaluronated imatinib liposomes with hybrid approach to target CD44 and P-gp overexpressing MDR cancer: an in-vitro, in-vivo and mechanistic investigation. *J. Drug Targeting* **2019**, *27*, 183−192.

(5) Dei, S.; Braconi, L.; Trezza, A.; Menicatti, M.; Contino, M.; Coronnello, M.; Chiaramonte, N.; Manetti, D.; Perrone, M. G.; Romanelli, M. N.; Udomtanakunchai, C.; Colabufo, N. A.; Bartolucci, G.; Spiga, O.; Salerno, M.; Teodori, E. Modulation of the spacer in N,N-bis(alkanol)amine aryl ester heterodimers led to the discovery of a series of highly potent P-glycoprotein-based multidrug resistance (MDR) modulators. *Eur. J. Med. Chem.* **2019**, *172*, 71−94.

(6) Li, S.; Zhao, Q.; Wang, B.; Yuan, S.; Wang, X.; Li, K. Quercetin reversed MDR in breast cancer cells through down-regulating P-gp expression and eliminating cancer stem cells mediated by YB-1 nuclear translocation. *Phytother. Res.* **2018**, *32*, 1530−1536.

(7) Zou, Z.; Zou, R.; Zong, D.; Shi, Y.; Chen, J.; Huang, J.; Zhu, J.; Chen, L.; Bao, X.; Liu, Y.; Liu, W.; Huang, W.; Hu, J.; Chen, Z.; Lao, X.; Chen, C.; Huang, X.; Lu, Y.; Ni, X.; Fang, D.; Wu, D.; Lu, S.; Jiang, M.; Qiu, C.; Wu, Y.; Qiu, Q.; Dong, Y.; Su, Y.; Zhao, C.; Zhong, Z.; Cai, J.; Liang, Y. miR-495 sensitizes MDR cancer cells to the combination of doxorubicin and taxol by inhibiting MDR1 expression. *J. Cell. Mol. Med.* **2017**, *21*, 1929−1943.

(8) Zhang, X.; Li, Y.; Wei, M.; Liu, C.; Yu, T. Cetuximab-modified silica nanoparticle loaded with ICG for tumor-targeted combinational therapy of breast cancer. *Drug Delivery* **2019**, *26*, 129−136.

(9) Meng, N.; Zhou, Z.; Chen, Q. c(RGDyK) Peptide-Conjugated Pluronic Micelle for the Effective Delivery of Epirubicin in Glioblastoma: Combination of Radiotherapy and Chemotherapy. *J. Biomater. Tissue Eng.* **2018**, *8*, 1551−1557.

(10) Zhao, X.; Tang, D.; Yang, T.; Wang, C. Facile preparation of biocompatible nanostructured lipid carrier with ultra-small size as a tumor-penetration delivery system. *Colloids Surf., B* **2018**, *170*, 355−363.

(11) Xiong, H.; Du, S.; Zhang, P.; Jiang, Z.; Zhou, J.; Yao, J. Primary tumor and pre-metastatic niches co-targeting "peptides-lego" hybrid hydroxyapatite nanoparticles for metastatic breast cancer treatment. *Biomater. Sci.* **2018**, *6*, 2591−2604.

(12) Li, M.; Luo, Z.; Zhao, Y. Self-Assembled Hybrid Nanostructures: Versatile Multifunctional Nanoplatforms for Cancer Diagnosis and Therapy. *Chem. Mater.* **2018**, *30*, 25−53.

(13) Wang, C.; Han, M.; Liu, X.; Chen, S.; Hu, F.; Sun, J.; Yuan, H. Mitoxantrone-preloaded water-responsive phospholipid-amorphous calcium carbonate hybrid nanoparticles for targeted and effective cancer therapy. *Int. J. Nanomed.* **2019**, *Volume 14*, 1503−1517.

(14) Wang, C.; Liu, X.; Chen, S.; Hu, F.; Sun, J.; Yuan, H. Facile preparation of phospholipid−amorphous calcium carbonate hybrid nanoparticles: toward controllable burst drug release and enhanced tumor penetration. *Chem. Commun.* **2018**, *54*, 13080−13083.

(15) Tang, D.; Zhao, X.; Yang, T.; Wang, C. Paclitaxel prodrug based mixed micelles for tumor-targeted chemotherapy. *RSC Adv.* **2018**, *8*, 380−389.

(16) Rao, L.; Bu, L.-L.; Cai, B.; Xu, J.-H.; Li, A.; Zhang, W.-F.; Sun, Z.-J.; Guo, S.-S.; Liu, W.; Wang, T.-H.; Zhao, X.-Z. Cancer Cell Membrane-Coated Upconversion Nanoprobes for Highly Specific Tumor Imaging. *Adv. Mater.* **2016**, *28*, 3460−3466.

(17) Chen, Z.; Zhao, P.; Luo, Z.; Zheng, M.; Tian, H.; Gong, P.; Gao, G.; Pan, H.; Liu, L.; Ma, A.; Cui, H.; Ma, Y.; Cai, L. Cancer Cell Membrane-Biomimetic Nanoparticles for Homologous-Targeting Dual-Modal Imaging and Photothermal Therapy. *ACS Nano* **2016**, *10*, 10049−10057.

(18) Cheng, C.; Meng, Y.; Zhang, Z.; Li, Y.; Liu, C.; Zhang, Q. pH responsible and fluorescent Cy5.5-PEG-g-A-HA/CDDP complex nanoparticles: synthesis, characterization, and application for targeted drug delivery. *J. Mater. Sci.: Mater. Med.* **2019**, *30*, 58.

(19) Tang, Q. S.; Chen, D. Z.; Xue, W. Q.; Xiang, J. Y.; Gong, Y. C.; Zhang, L.; Guo, C. Q. Preparation and biodistribution of Re-188-labeled folate conjugated human serum albumin magnetic cisplatin nanoparticles (Re-188-folate-CDDP/HSA MNPs) in vivo. *Int. J. Nanomed.* **2011**, *6*, 3077−3085.

(20) Tu, X.; Min, L.-F.; Chen, Q.; Xie, M.-X.; He, L.-L. Study on Using Magnetic Iron Oxide Nanoparticles as HIF-1 alpha shRNA Gene Carrier to Reverse Cisplatin Resistance of A549/CDDP Cell Lines. *Prog. Biochem. Biophys.* **2010**, *37*, 1090−1100.

(21) Bao, X.; Gao, M.; Xu, H.; Liu, K.-X.; Zhang, C.-H.; Jiang, N.; Chu, Q.-C.; Guan, X.; Tian, Y. A novel oleanolic acid-loaded PLGA-TPGS nanoparticle for liver cancer treatment. *Drug Dev. Ind. Pharm.* **2015**, *41*, 1193−1203.

DOI: 10.1021/acsomega.9b02261
ACS Omega 2020, 5, 995−1002

(22) Man, D. K. W.; Casettari, L.; Cespi, M.; Bonacucina, G.; Palmieri, G. F.; Sze, S. C. W.; Leung, G. P. H.; Lam, J. K. W.; Kwok, P. C. L. Oleanolic Acid Loaded PEGylated PLA and PLGA Nanoparticles with Enhanced Cytotoxic Activity against Cancer Cells. *Mol. Pharmaceutics* **2015**, *12*, 2112−2125.
(23) Shanmugam, M. K.; Dai, X.; Kumar, A. P.; Tan, B. K. H.; Sethi, G.; Bishayee, A. Oleanolic acid and its synthetic derivatives for the prevention and therapy of cancer: Preclinical and clinical evidence. *Cancer Lett.* **2014**, *346*, 206−216.
(24) Tan, L.; Ma, B.; QianZhao; LanZhang; Chen, L.; Peng, J.; Qian, Z. Toxicity Evaluation and Anti-Tumor Study of Docetaxel Loaded mPEG-Polyester Micelles for Breast Cancer Therapy. *J. Biomed. Nanotechnol.* **2017**, *13*, 393−408.
(25) Wen, L.; Liang, C.; Chen, E.; Chen, W.; Liang, F.; Zhi, X.; Wei, T.; Xue, F.; Li, G.; Yang, Q.; Gong, W.; Feng, X.; Bai, X.; Liang, T. Regulation of Multi-drug Resistance in hepatocellular carcinoma cells is TRPC6/Calcium Dependent. *Sci. Rep.* **2016**, *6*, 23269.
(26) Sun, S.; Gebauer, D.; Cölfen, H. A solvothermal method for synthesizing monolayer protected amorphous calcium carbonate clusters. *Chem. Commun.* **2016**, *52*, 7036−7038.
(27) Vilella, A.; Ruozi, B.; Belletti, D.; Pederzoli, F.; Galliani, M.; Semeghini, V.; Forni, F.; Zoli, M.; Vandelli, M.; Tosi, G. Endocytosis of Nanomedicines: The Case of Glycopeptide Engineered PLGA Nanoparticles. *Pharmaceutics* **2015**, *7*, 74−89.
(28) Davis, F. M.; Azimi, I.; Faville, R. A.; Peters, A. A.; Jalink, K.; Putney, J. W., Jr.; Goodhill, G. J.; Thompson, E. W.; Roberts-Thomson, S. J.; Monteith, G. R. Induction of epithelial-mesenchymal transition (EMT) in breast cancer cells is calcium signal dependent. *Oncogene* **2014**, *33*, 2307−2316.
(29) Wang, C.; Li, M.; Yang, T.; Ding, X.; Bao, X.; Ding, Y.; Xiong, H.; Wu, Y.; Wang, W.; Zhou, J. A self-assembled system for tumor-targeted co-delivery of drug and gene. *Mater. Sci. Eng., C* **2015**, *56*, 280−285.
(30) Hu, Z.; Deng, Y. Superhydrophobic Surface Fabricated from Fatty Acid-Modified Precipitated Calcium Carbonate. *Ind. Eng. Chem. Res.* **2010**, *49*, 5625−5630.
(31) Semalty, A.; Semalty, M.; Rawat, B. S.; Singh, D.; Rawat, M. Pharmacosomes: the lipid-based new drug delivery system. *Expert Opin. Drug Delivery* **2009**, *6*, 599−612.
(32) Wang, C.; Bao, X.; Ding, X.; Ding, Y.; Abbad, S.; Wang, Y.; Li, M.; Su, Y.; Wang, W.; Zhou, J. A multifunctional self-dissociative polyethyleneimine derivative coating polymer for enhancing the gene transfection efficiency of DNA/polyethyleneimine polyplexes in vitro and in vivo. *Polym. Chem.* **2015**, *6*, 780−796.
(33) Gao, F.; Zhang, J.; Fu, C.; Xie, X.; Peng, F.; You, J.; Tang, H.; Wang, Z.; Li, P.; Chen, J. iRGD-modified lipid-polymer hybrid nanoparticles loaded with isoliquiritigenin to enhance anti-breast cancer effect and tumor-targeting ability. *Int. J. Nanomed.* **2017**, *Volume 12*, 4147−4162.
(34) Natarajan, A.; Gruettner, C.; Ivkov, R.; DeNardo, G. L.; Mirick, G.; Yuan, A.; Foreman, A.; DeNardo, S. J. NanoFerrite particle based radioimmunonanoparticles: binding affinity and in vivo pharmacokinetics. *Bioconjugate Chem.* **2008**, *19*, 1211−1218.
(35) Chai, S.; Kan, S.; Sun, R.; Zhou, R.; Sun, Y.; Chen, W.; Yu, B. Fabricating polydopamine-coated MoSe2-wrapped hollow mesoporous silica nanoplatform for controlled drug release and chemo-photothermal therapy. *Int. J. Nanomed.* **2018**, *Volume 13*, 7607−7621.
(36) Wang, C.; Chen, S.; Yu, Q.; Hu, F.; Yuan, H. Taking advantage of the disadvantage: employing the high aqueous instability of amorphous calcium carbonate to realize burst drug release within cancer cells. *J. Mater. Chem. B* **2017**, *5*, 2068−2073.
(37) Yalçın, S.; Ozluer, O.; Gunduz, U. Nanoparticle-based drug delivery in cancer: the role of cell membrane structures. *Ther. Delivery* **2016**, *7*, 773−781.
(38) Khan, M. W.; Zhao, P.; Khan, A.; Raza, F.; Raza, S. M.; Sarfraz, M.; Chen, Y.; Li, M.; Yang, T.; Ma, X.; Xiang, G. Synergism of cisplatin-oleanolic acid co-loaded calcium carbonate nanoparticles on hepatocellular carcinoma cells for enhanced apoptosis and reduced hepatotoxicity. *Int. J. Nanomed.* **2019**, *Volume 14*, 3753−3771.
(39) Xiong, H.; Wu, Y.; Jiang, Z.; Zhou, J.; Yang, M.; Yao, J. pH-activatable polymeric nanodrugs enhanced tumor chemo/antiangiogenic combination therapy through improving targeting drug release. *J. Colloid Interface Sci.* **2019**, *536*, 135−148.

DOI: 10.1021/acsomega.9b02261
ACS Omega 2020, 5, 995−1002